Design of optimal switching surfaces for switched autonomous systems

Axel Schild, Xu Ding, Magnus Egerstedt and Jan Lunze

Abstract— **This paper presents a novel, computationally feasible procedure for computing optimal switching surfaces, i.e. optimal feedback controllers for switched autonomous nonlinear systems. The systems under consideration are regulated by appropriately scheduling their operation modes. Given a finite mode sequence, the control task requires to determine switching surfaces, which implicitly encode the optimal switching times for a family of trajectories emerging from a prespecified initial state set. Optimality of the switching times is assessed according to a nonlinear performance criterion.**

I. INTRODUCTION

Optimal control of switched systems attracted a considerable amount of attention over last few decades, mainly because such systems are found in many application domains such as robotics, power electronics, process engineering and manufacturing systems [13], [19], [21]. Switched systems consist of a continuous plant, whose output is to be regulated through discrete-valued control inputs that switch the plant among its available operation modes. In many practical applications, the mode sequence follows uniquely from the plant set-up and the control objective. In this case, the *switching times* constutite the *sole control influence*.

Switching time optimization [13], [20], [23] addresses the problem of determining optimal transition times for a given mode sequence and a particular initial state off-line, such that the state trajectory, which results from the *open-loop control* of the plant, minimizes a prespecified objective function. Due to non-convexity of the optimization problem, locally optimal switching times are the best, one can hope for.

To resolve sensitivity issues inherent to open-loop control, two different strategies have been pursued in the past. On the one hand, [3], [8] proposed *explicit* closed-loop control by means of an event generator that implements parametrized switching surfaces to trigger mode transitions. The fact that most of the computational effort is shifted to the off-line phase makes this design approach perfectly suited for the control of fast switching systems, like power converters. As a central drawback, tractability of the design problem requires to characterize the surface shape is a-priori in terms of a finite number of parameters, which are subsequently tuned with respect to a *single* reference trajectory or a family of trajectories. In this context, it is incorrect to speak of optimal switching surfaces, as only the parameter set is locally optimal. Besides this, it requires a large insight into the problem at hand in order to find a suitable parametrization heuristically.

An alternative route to feedback control was taken in [12], [22], which focus on solving the finite horizon nonlinear optimal control problem in real-time during the system operation. Here, the feedback law is specified implicitly as the solution to the real-time optimization problem. Compared to the explicit feedback approach, real-time optimal control requires less insight into the problem and generally results in a better system performance. These benefits, however, come at the price of a high computational complexity, no convergence or optimality guarantees and the inability to compensate disturbances, which perturb the system right before a mode transition is about to occur, due to the finite update rate of the switching times. Overall, this approach is best suited for slow switching systems, which are affected by low-frequency disturbances.

As the first of its kind, this paper provides a fundamental step for merging explicit and implicit optimal feedback control strategies into a unified framework, which exhibits beneficial properties of both worlds (see Fig. 1). Its central contribution is a novel, computationally viable framework for systematically approximating locally *optimal switching surfaces* of a switched autonomous system up to arbitrary precision by means of simplex meshes. The computationally demanding mesh generation is performed prior to system operation and the result is stored in the form of a look-up table. At run-time, evaluating the feedback law only requires to detect intersections between the state trajectory and these polytopical surfaces, which can be conducted fast and reliably.

In contrast to [8], the method proposed herein *does not* requires to fix the number of surface parameters a-priori. Instead, all surfaces are incrementally grown around initial seed points, such that the number of parameters, which are required to represent the optimal surfaces with desired accuracy, are autonomously decided by the algorithm at run-time. A remarkable feature of this approach is that is ensures optimality for each individual trajectory emerging from the given initial set, which is *rarely* the case for the surfaces derived according to [8]. Moreover, the generation of new mesh vertices is systematically guided by exploiting tangent plane information, which allows to maintain the computational burden as low as possible and distinguishes our approach from the procedure in [7].

The paper is structured as follows: Sect. 2 summarizes the system model and the optimal control problem. Sect. 3 establishes novel necessary and sufficient conditions for the existence of stationary optimal switching surfaces. All steps

A. Schild and J. Lunze are with Faculty of Electrical Engineering and Information Sciences, Ruhr-Universiteat Bochum, 44780 Bochum, Germany {lunze,schild}@atp.rub.de

X. Ding and M. Egerstedt are with the School of Electrical and Computer Engineering, Georgia Institute of Technology, Atlanta, GA 30332, USA {ding,magnus}@ece.gatech.edu

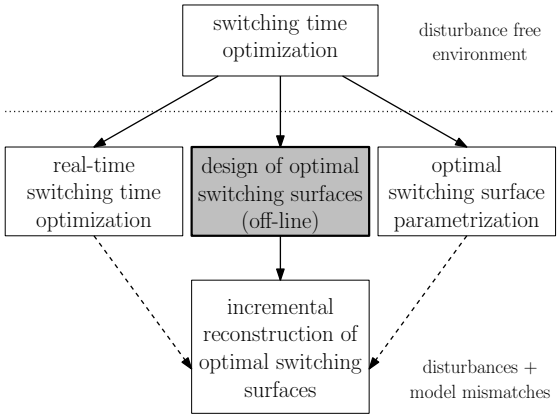

Fig. 1. Optimal feedback approaches for switched autonomous systems. The solution of the intermediate step (grey box) is adressed in this paper.

of the algorithm, which achieves to approximate the optimal surfaces through successive polygonization, are presented in detail in Sect. 4. The applicability and the performance of the design procedure is finally demonstrated at a simple robot example in Sect. 5.

II. PROBLEM FORMULATION FOR BIMODAL SWITCHED AUTONOMOUS SYSTEMS

For the sake of simplicity and clarity of presentation, the following sections focus on bimodal autonomous switched-mode dynamical systems

$$\dot{\boldsymbol{x}}(t) = \begin{cases} \boldsymbol{f}_0(\boldsymbol{x}(t)) & \text{if } t \in [t_0, \tau] \\ \boldsymbol{f}_1(\boldsymbol{x}(t)) & \text{if } t \in [\tau, t_f]\tau \end{cases} \quad . \tag{1}$$

which undergo a single mode transition $0 \to 1$ at a freely decidable *switching time* τ. Yet, all result naturally extend to autonomous hybrid systems with N autonomous as well as controlled switchings and state jumps.

In (1), $\boldsymbol{x} \in \mathbb{R}^n$ represents the continuous state and $\boldsymbol{f}_i$ is the smooth vector field, the *modal function*, associated with each operation mode. The state value $\boldsymbol{x}_1 = \boldsymbol{x}(\tau)$ corresponding to the switching time τ is referred to as the *switch point*. The time span $\delta_0 = \tau - t_0$ constitutes the *activation duration* of mode one, while $\delta_1 = t_f - \tau$ defines the activation duration of the second mode two. Note, that the final time t_f is free. Denote the *activation duration sequence* by $\bar{\delta} = (\delta_0, \delta_1)$, the *terminal point* as $\boldsymbol{x}_2 = \boldsymbol{x}(t_f)$ and the resulting *switch point sequence* as $\bar{\boldsymbol{x}} = (\boldsymbol{x}_0, \boldsymbol{x}_1, \boldsymbol{x}_2)$.

Definition 1: For any initial state $\boldsymbol{x}_0$, the expression $\boldsymbol{x}_{[t_0,t_f]}(t, \boldsymbol{x}_0, \tau)$ refers to the state trajectory, which departs from $\boldsymbol{x}(t_0) = \boldsymbol{x}_0$ and sequentially evolves according to $\boldsymbol{f}_k$ for δ_k time units. Whenever clear from the context, $\boldsymbol{x}_{[t_0,t_f]}(t, \boldsymbol{x}_0, \tau)$ is abbreviated by $\boldsymbol{x}_{[t_0,t_f]})(t)$.

The task addressed in this paper is to determine *stationary optimal switching surfaces*, which enable an optimal, closed-loop operation of the switched system.

Definition 2: A *switching surface* is a compact set

$$\mathcal{M}_{10} = \{\boldsymbol{x} \,:\, \Phi_{10}(\boldsymbol{x}) = 0\} \quad , \tag{2}$$

in the state space of codimension-1, which is implicitly defined through an *event function* Φ_{10}. A trajectory starting at $\boldsymbol{x}_0$ under mode zero triggers the transition $0 \to 1$ at the time $\tau(\mathcal{M}_{10}, \boldsymbol{x}_0)$, at which it first intersects $\mathcal{M}_{10}$, i.e. $\Phi_{10}(\boldsymbol{x}(\tau(\mathcal{M}_{10}, \boldsymbol{x}_0))) = 0$ and $\Phi_{10}(\boldsymbol{x}(t)) \neq 0$, $\forall t \in [t_0, \tau)$. All subsequent intersections of $\mathcal{M}_{10}$ under the evolution of mode one have no effect on the system.

In analogy to the above, the union of all terminal points $\boldsymbol{x}_2$ forms the *terminal surface* $\mathcal{M}_{T1}$. Under autonomous switching, or more precisely *closed-loop switching*, the switching time $\tau(\mathcal{M}_{10}, \boldsymbol{x}_0)$, the switch point $\boldsymbol{x}_1(\mathcal{M}_{10}, \boldsymbol{x}_0)$ and the activation duration $\delta_0(\mathcal{M}_{10}, \boldsymbol{x}_0)$ are all explicit functions of the initial state and the triggering surfaces. To prevent notational clutter, these arguments are dropped whenever they are clear from the context.

Optimality of a switching surfaces $\mathcal{M}_{10}$ is assessed on the basis of a user-defined nonlinear performance criterion. An individual trajectory $\boldsymbol{x}_{[t_0,t_f]}(t)$ is optimal, iff it minimizes a cost functional of the form

$$\tilde{J}(\bar{\delta}, \boldsymbol{x}_0) = \int_{t_0}^{\tau(\mathcal{M}_{10}, \boldsymbol{x}_0)} L_0(\boldsymbol{x}(t))\,\mathrm{d}t + \int_{\tau(\mathcal{M}_{10}, \boldsymbol{x}_0)}^{t_f(\mathcal{M}_{T1}, \boldsymbol{x}_0)} L_1(\boldsymbol{x}(t))\,\mathrm{d}t + \phi_1(\boldsymbol{x}_1) \quad . \tag{3}$$

Here, the piecewise-defined stage costs L_i penalize the transient evolution, while ϕ_i accounts for potential switching costs. Optimality of a *switching surface configuration* $\bar{\mathcal{M}} = \{\mathcal{M}_{10}, \mathcal{M}_{T1}\}$, on the other hand, is defined with respect to a whole family of trajectories.

Problem 1: **Given** a bimodal switched-mode system (1), as well as initial and terminal regions $\mathcal{X}_0$ and $\mathcal{X}_T$, **determine** the optimal surface configuration $\bar{\mathcal{M}}^\star$, which minimizes the nonlinear performance criterion

$$J(\bar{\mathcal{M}}, \mathcal{X}_0) = \int_{\mathcal{X}_0} \tilde{J}(\delta\left(\bar{\mathcal{M}}, \boldsymbol{x}_0\right), \boldsymbol{x}_0)\mathrm{d}\boldsymbol{x}_0 \tag{4}$$

with respect to the constraints (1) and

$$\delta_k(\bar{\mathcal{M}}, \boldsymbol{x}_0) \;\geq 0 \tag{5}$$

$$\boldsymbol{\psi}\left(\boldsymbol{x}_2^\star(\bar{\mathcal{M}}, \boldsymbol{x}_0)\right) \leq \mathbf{0} \quad . \tag{6}$$

for all $\boldsymbol{x}_0 \in \mathcal{X}_0$. The terminal constraints (6) encode the shape of the terminal region $\mathcal{X}_T$.

Prob. 1 is infinite-dimensional, non-convex and constrained, as the optimization is conducted over the set of all feasible event functions, which ensure satisfaction of the inequality constraints (5). Thus, locally optimal manifolds are the best, one can hope for.

Definition 3: Given an initial set $\mathcal{X}_0$, the set $\mathcal{M}(\mathcal{X}_0)$ of *feasible surface configurations* contains all elements $\bar{\mathcal{M}}$, which generate state trajectories $\boldsymbol{x}_{[t_0,t_f]}(t, \boldsymbol{x}_0, \tau(\bar{\mathcal{M}}, \boldsymbol{x}_0))$ for all $\boldsymbol{x}_0 \in \mathcal{X}_0$ with strictly positive activation durations.

Definition 4: Prob. 1 is called *non-degenerated*, iff the optimal surface configuration $\bar{\mathcal{M}}^\star$ lies in the interior of the feasible set $\mathcal{M}(\mathcal{X}_0)$, i.e. (5) is not in force.

Degeneracency of Prob. 1 implies that either a section of the initial set boundary $\partial\mathcal{X}_0$ constitutes a part of the optimal switching surface, or $\mathcal{M}_{10}^\star$ and $\mathcal{M}_{T1}^\star$ merge inside the terminal set $\mathcal{X}_T$, or both. Regarding the first case, the configuration $\bar{\mathcal{M}}^\star$ generates a family of trajectories $\boldsymbol{x}_{[t_0,t_f]}(t, \boldsymbol{x}_0, \tau(\bar{\mathcal{M}}^\star, \boldsymbol{x}_0))$, which are not optimal with respect to (3). Those trajectories emanate from a n-dimensional subset $\mathcal{X}_0^0 \subseteq \mathcal{X}_0$ of initial

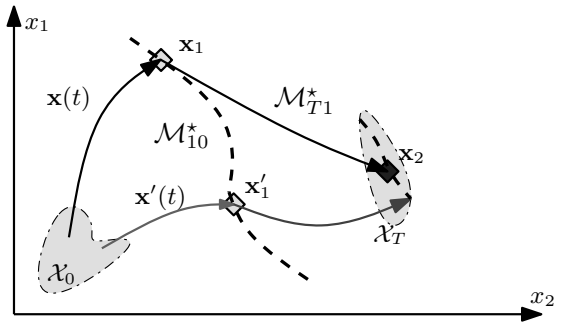

Fig. 2. State space plot of sample executions $\boldsymbol{x}(t)$ over one switchings.

states and all require a vanishing first activation duration. The latter, however, contradicts the definition 2 of a switching surface. The second case is similar, but the optimal trajetory only evolve according to mode zero, while mode one is never activated. While degeneracency does not require conceptual changes to solve Prob. 1, it would complicate the presentation of the remaining sections. Thus, Prob. 1 is assumed to be non-degenerated throughout the rest of the paper.

Inequality constraints (6) require the terminal mainfold to be contained inside a given *terminal region* $\mathcal{X}_T$. To rule out infeasibility of Prob. 1, the regions $\mathcal{X}_0$ and $\mathcal{X}_T$ are assumed to be consistent and non-overlapping, i.e. $\mathcal{X}_0 \cap \mathcal{X}_T = \emptyset$.

Definition 5: The forward reachable tube

$$\mathcal{F}^\star(\mathcal{X}_0) = \{\boldsymbol{y} \,|\, \exists \boldsymbol{x}_0 \in \mathcal{X}_0,\, \tau \geq 0,\, t \geq \tau,\, \boldsymbol{x}_{[t_0,\infty]}(t, \boldsymbol{x}, \tau) = \boldsymbol{y}\}$$

contains all states $\boldsymbol{y}$ can be reached a optimal trajectory emanating from $\mathcal{X}_0$ under the switch dynamics (1).

Definition 6: A pair $(\mathcal{X}_0, \mathcal{X}_T)$ of initial and terminal regions is called consistent with respect to (1), if $\mathcal{X}_T \in \mathcal{F}^\star(\mathcal{X}_0)$ is completely contained in the forward reachable tube of $\mathcal{X}_0$. Fig. 2 illustrates the considered problem setting in state-space. Both depicted sample trajectories emanate from $\mathcal{X}_0$ and intersect the surface $\mathcal{M}^\star_{10}$ in switch points $\boldsymbol{x}^\star_1$, $\boldsymbol{x}'^\star_1$, such that both evolutions governed by mode two eventually enter the terminal region $\mathcal{X}_T$. Besides these optimal points, there obviously exist infinitely many alternative points along both trajectories $\boldsymbol{x}^\star(t)$ and $\boldsymbol{x}'^\star(t)$, for which the latter will enter the terminal region. However, switching at any points other than $\boldsymbol{x}^\star_1$, $\boldsymbol{x}'^\star_1$ will incur higher costs.

Remark 1: In contrast to most existing literature on optimal control of switched autonomous systems, the control problem 1 is cast over a variable time horizon, which is crucial for the existence of stationary optimal switching surfaces.

Remark 2: We specifically incorporate terminal inequality constraints into Prob. 1, as such terminal constraints are essential for attacking the on-line reconstruction of optimal switching surfaces, which is the ultimate goal of this research.

III. EXISTENCE OF STATIONARY OPTIMAL SWITCHING SURFACES

As stated in Prob. 1, the design task is to find a configuration of *stationary* optimal surfaces, which encode all optimal activation duration $\delta^\star_k(\boldsymbol{x}_0)$, i.e. the optimal switch point $\boldsymbol{x}^\star_k(\boldsymbol{x}_0)$ for all $\boldsymbol{x}_0 \in \mathcal{X}_0$. *Stationariness* of these surfaces is paramount for tractability of the problem, but is not necessarily given, in particular not, if the final time t_f is fix [7]. Thus, a fundamental concern is to identify the class of optimal control problems, which admit such a stationary configuration. The subsequent discussion focusses on the switching surface $\mathcal{M}^\star_{10}$. By the same arguments stationariness of the terminal surface can be verified.

The implicit representation (2) of the optimal surface by means of a switching condition is clearly not unique. One particular insightful representation of $\mathcal{M}^\star_{10}$ employs the *unique* event function

$$\delta^\star_0(\boldsymbol{x}) = \Phi^\star_{10}(\boldsymbol{x}) \quad , \tag{7}$$

which returns the optimal activation duration $\delta^\star_0(\boldsymbol{x})$ for any $\boldsymbol{x}$. Obviously, if $\Phi^\star_{10}$ exists, it constitutes a *time-invariant* optimal feedback law for the first activation duration.

Proposition 1: A stationary optimal surface $\mathcal{M}^\star_{10}$, which solve the optimal control problem (4)-(5), exist, iff Prob. 1 admits *time-invariant* state-feedback laws for the optimal activation durations $\delta^\star_0$.

Proof: **Necessity:** Suppose that the optimal state-feedback law (7) for the first activation duration is time-varying. Then there exists a time $t'_0 \neq t_0$ and a state $\boldsymbol{x}_0$, so that the event function $\Phi^\star_{10}\left(\boldsymbol{x}_0, t'_0\right) \neq \Phi^\star_{10}(\boldsymbol{x}_0, t_0) > 0$ returns two different optimal activation durations for the first mode. Due to autonomy and time-invariance of the mode dynamics (1) both optimal trajectories $\boldsymbol{x}^\star_{[t_0,t_f]}(t, \boldsymbol{x}_0, \tau)$ and $\boldsymbol{x}'^\star_{[t'_0,t'_f]}(t, \boldsymbol{x}_0, \tau')$ must switch at two different points $\boldsymbol{x}_1 \neq \boldsymbol{x}'_1$, which contradicts stationariness of the optimal surface $\mathcal{M}^\star_{10}$.

Sufficiency: follows from inverting the arguments of the previous paragraph. ■

Clearly, not all optimal control problems admit a time-invariant optimal feedback law.

Proposition 2: The optimal control problem (4)-(5) admits a stationary optimal switching surface $\mathcal{M}^\star_{10}$, if the final time t_f is unspecified and the cost and constraint components L_i, ϕ_i and ψ are smooth, time-invariant functions.

Proof: By Bellman's principle of optimality [4], an optimal trajectory $\boldsymbol{x}^\star_{[t_0,t_f]}(t, \boldsymbol{x}_0, \tau)$ can be arbitrarily subdivided into two parts for some δ', where the trailing section $\boldsymbol{x}^\star_{[t_0+\delta',t_f]}(t, \boldsymbol{x}^\star(t_0+\delta'), \tau)$ minimizes the costs-to-go $\tilde{J}^\star(\bar{\delta}'^\star, \boldsymbol{x}^\star(t_0+\delta')$. Given $\delta' \leq \delta^\star_0$ the performance index

$$\tilde{J}^\star(\bar{\delta}^\star, \boldsymbol{x}_0) = \int_{t_0}^{t_0+\delta'} L_0(\boldsymbol{x}(t))\,\mathrm{d}t + \int_{t_0+\delta'}^{t_0+\delta^\star_0} L_0(\boldsymbol{x}(t))\,\mathrm{d}t + \phi_1\left(\boldsymbol{x}^\star_1\right) + \int_{t_0+\delta^\star_0}^{t_0+\delta^\star_0+\delta^\star_1} L_1(\boldsymbol{x}(t))\,\mathrm{d}t.$$

can be split up into two parts. If both L_i and ϕ are time-invariant, shifting the integration bounds by δ' yields

$$\tilde{J}^\star(\bar{\delta}'^\star, \boldsymbol{x}'_0) = \int_{t_0}^{t_0+\delta^\star_0-\delta'} L_0(\boldsymbol{x}(t+\delta'))\,\mathrm{d}t + \phi_1\left(\boldsymbol{x}^\star_1\right) + \int_{t_0+\delta^\star_0-\delta'}^{t_0+\delta^\star_0-\delta'+\delta^\star_1} L_1(\boldsymbol{x}(t+\delta'))\,\mathrm{d}t,$$

which corresponds to the optimal costs incurred by $\boldsymbol{x}^\star_{[t_0,t_f-\delta']}(t, \boldsymbol{x}'_0, \tau^\star-\delta')$. As δ' is arbitrary, the optimal feedback law for $\delta^\star_0$ must be time-invariant and Prop. 1 ensures stationariness of $\mathcal{M}^\star_{10}$. ■

Remark 3: As emphazised in Prop. 2, casting the Prob. 1 over a variable time horizon is only necessary but not

sufficient for stationariness of $\mathcal{M}_{10}^{\star}$. If at least on of the cost or constraint components explicitly depends on time in a nonlinear way, then a time-shift of δ' is almost always impossible and Bellman's principle precludes the existence of stationary optimal surfaces $\mathcal{M}_{10}^{\star}$.

IV. PIECEWISE-AFFINE APPROXIMATION OF THE OPTIMAL SWITCHING SURFACE

A. Polygonization of implicit surfaces

It is clear that minimizing the non-convex cost functional (4) over the surface configuration $\bar{\mathcal{M}}$ is comparable to solving the HJB-equation of the associated switching time optimization problem, which is intractable. To relax Prob. 1 we, therefore, propose to approximate the true optimal event functions $\Phi_{10}^{\star}$, $\Phi_{T1}^{\star}$ of both surfaces by sufficiently accurate piecewise-affine functions $\tilde{\Phi}_{10}^{\star}$, $\tilde{\Phi}_{T1}^{\star}$. Here, all effort can be concentrated to a neighborhood around the true optimal $\mathcal{M}_{k+1,k}^{\star}$, where $\Phi_{k+1,k}^{\star} = 0$. Moreover, it suffices to recover surface patches, as all trajectories of interest emerge from a bounded initial set $\mathcal{X}_0$ and only visit a small fraction of the state space.

The incremental generation of $\tilde{\Phi}_{k+1,k}^{\star}$ in the region of interest can be achieved by *polygonalizing* the *implicit surface* $\mathcal{M}_{k+1,k}^{\star}$. Polygonization represents a mature interdisciplinary research field of computer graphics and numerical continuation. It aims at systematically covering a functionally specified, complex-shaped surface (2) by a simplex mesh. The simplex vertices need to be successively sampled along the surface, such that accuracy bounds are met. Marching triangle algorithms [15], [17], [18] and other predictor-corrector continuation methods [2], [6], [16] exhibits properties, which are prefect for the design task at hand:

- These procedures explore only the relevant state space fraction by employing tangent information of the true surface.
- The successive polygonization allows to restrict the surface construction to the region of interest.
- By varying the vertex distance, it is possible to actively control the approximation precision. Small simplices ensure an accurate representation of regions with high "curvature", whereas flat sections can be broadly covered by large simplices.

All feature help to reduce the computational complexity significantly, which is crucial for applicability of the approach. As gridding becomes prohibitively expensive with an increasing number of state space dimensions, only one or two-dimensional surfaces can be reconstructed with acceptable effort in practise. In summary, all successive polygonization algorithms repeatedly execute three basic operations:

1) determination of an anchor point $\boldsymbol{x}_{(k+1)j}^{\star} \in \mathcal{M}_{(k+1)k}^{\star}$,
2) determination of the tangent plane $\mathcal{T}_{(k+1)k}^{\star}(\boldsymbol{x}_{(k+1)j}^{\star})$.
3) projection of so called candidate sample points $\boldsymbol{x}_{(k+1)i} \in \mathcal{T}_{(k+1)k}^{\star}(\boldsymbol{x}_{(k+1)j}^{\star})$ to generate new anchor points.

They require to solve a constrained switching time optimization problem similar to [13]. The following sections summarize the details for performing this switching time optimization. In particular, it is explained how to obtain the tangent plane $\mathcal{T}_{(k+1)k}^{\star}(\boldsymbol{x}_{(k+1)i}^{\star})$ as a by-product, if the optimization is executed by second order methods [9].

Remark 4: Critical assumptions of any predictor-corrector continuation method are that the implicit surface (2) is continuous, its defining event function $\Phi_{(k+1)k}(\boldsymbol{x}_0)$ is differentiable and $\|\mathrm{d}\Phi_{(k+1)k}(\boldsymbol{x})/\mathrm{d}\boldsymbol{x}\| \neq 0$ at all $\boldsymbol{x} \in \mathcal{M}_{(k+1)k}^{\star}$. Under these assumptions, the polygonal approximation converges to the true surface with a decreasing mesh size [1]. It will be shown later in Sect. IV-D, that locally optimal surfaces $\mathcal{M}_{10}^{\star}$ and $\mathcal{M}_{T1}^{\star}$ satisfy these properties.

B. Switching time optimization via nonlinear programming

The application of Lebesgue sampling to the original problem, i.e. the discretization of the continuous dynamics (1) and the performance criterion (4) with respect to the *unknown* switching time τ and the terminal time t_f, allows to transform Prob. 1 into an ordinary discrete-time optimal control problem. This reformulation is extremely useful, as it does not only open up the large toolkit of classical optimal control, but also reveals valuable insight into the problem at hand. Such a *discrete-event perspective* on optimal control of switched systems was previously proposed in [14], [23], however, without fully exploiting or interpreting the structure hidden in the discretized dynamics. An exact discretization

$$\tilde{J}(\bar{\delta}, \boldsymbol{x}_0) = \sum_{k=0}^{1} g_k(\boldsymbol{x}_k, \delta_k) \tag{8}$$

$$\boldsymbol{x}_{k+1} = \boldsymbol{h}_k(\boldsymbol{x}_k, \delta_k)\,, \quad \boldsymbol{x}_0 = \boldsymbol{x}(t_0) \tag{9}$$

of the dynamics and the cost function requires the symbolic integration of

$$\boldsymbol{h}_k(\boldsymbol{x}_k, \delta_k) = \boldsymbol{x}_k + \int_0^{\delta_k} \boldsymbol{f}_k(\boldsymbol{x}(t))\,\mathrm{d}t$$

$$g_k(\boldsymbol{x}_k, \delta_k) = \begin{cases} \int_0^{\delta_0} L_0(\boldsymbol{x}(t_0+t))\,\mathrm{d}t & \text{if } k = 0 \\ \int_0^{\delta_1} L_1(\boldsymbol{x}(t_0+\delta_0+t))\,\mathrm{d}t + \phi(\boldsymbol{x}_1) & \text{otherwise} \end{cases},$$

which is rarely possible. Nevertheless, we can derive explicit expressions for the partial derivatives of $g_k(\boldsymbol{x}_k, \delta_k)$ and $h_k(\boldsymbol{x}_k, \delta_k)$ (see appendix A), which are need for the switching time optimization. In particular, the first partial derivatives of discretized dynamics $h_k(\boldsymbol{x}_k, \delta_k)$ are

$$\boldsymbol{A}_k = \frac{\partial \boldsymbol{h}_k}{\partial \boldsymbol{x}}(\boldsymbol{x}_k, \delta_k) = \boldsymbol{Z}_k(\delta_k) \tag{10}$$

$$\boldsymbol{B}_k = \frac{\partial \boldsymbol{h}_k}{\partial \delta}(\boldsymbol{x}_k, \delta_k) = \boldsymbol{f}_k(\boldsymbol{x}_{k+1})\ , \tag{11}$$

where the state transition matrix $\boldsymbol{Z}_k(t)$ follows from simultaneous integration of

$$\dot{\boldsymbol{\zeta}}(t) = \boldsymbol{f}_k(\boldsymbol{\zeta}(t))\,, \quad \boldsymbol{\zeta}(0) = \boldsymbol{x}_k$$

$$\dot{\boldsymbol{Z}}_k(t) = \frac{\partial \boldsymbol{f}_k}{\partial \boldsymbol{\zeta}}(\boldsymbol{\zeta}(t))\,\boldsymbol{Z}_k(t)\,, \quad \boldsymbol{Z}(0) = \boldsymbol{I}\ .$$

By imposing specific initial conditions $\boldsymbol{x}_0 \in \mathcal{X}_0$ onto the system (1), the discretization (8), (9) translates the

constrained switching time optimization problem

$$\min_{\tau,t_f} \int_{t_0}^{\tau} L_0(\boldsymbol{x}(t))\,\mathrm{d}t + \int_{\tau}^{t_f} L_1(\boldsymbol{x}(t))\,\mathrm{d}t + \phi_1(\boldsymbol{x}_1) \quad \text{subject to}$$
$$\dot{\boldsymbol{x}}(t) = \boldsymbol{f}_k(\boldsymbol{x}(t))$$
$$\delta_k \geq 0,\ \forall k,\ \ \boldsymbol{\psi}(\boldsymbol{x}_2) \leq \mathbf{0}\ ,$$

which is associated with Prob. 1, into an ordinary constrained nonlinear discrete-time optimal control problem

$$\min_{\bar{\delta}} \tilde{J}(\bar{\delta}, \boldsymbol{x}_0) = \sum_{k=0}^{1} g_k(\boldsymbol{x}_k, \delta_k) \quad \text{subject to} \tag{12}$$
$$\boldsymbol{x}_{k+1} = \boldsymbol{h}_k(\boldsymbol{x}_k, \delta_k) \tag{13}$$
$$\tau_k \geq 0,\ \boldsymbol{\psi}(\boldsymbol{x}_2) \leq \mathbf{0} \tag{14}$$

in terms of the activation durations δ_k, which is well understood and can be iteratively solved via sequential quadratic programming (SQP) [11]. The central idea behind SQP is to expand the cost function $\tilde{J}(\bar{\delta}^{(i)} + \Delta\bar{\delta}, \boldsymbol{x}_0)$ at the i-th iteration around the current guess $\bar{\delta}^{(i)}, \bar{\boldsymbol{x}}^{(i)}$ up to second order and to minimize the expression

$$\Delta\tilde{J}(\Delta\bar{\delta}) = \frac{\partial \tilde{J}}{\partial \bar{\delta}}\Big(\bar{\delta}^{(i)}, \boldsymbol{x}_0\Big)\Delta\bar{\delta} + \Delta\bar{\delta}^{\mathrm{T}} \frac{\partial^2 \tilde{J}}{\partial \bar{\delta}^2}\Big(\bar{\delta}^{(i)}, \boldsymbol{x}_0\Big)\Delta\bar{\delta}$$

with respect to $\Delta\bar{\delta}$. The minimizer $\Delta\bar{\delta}^{\star}$ is obtained as a solution to an associated conventional LQR problem by means of interior point methods and constitutes the *newton descent direction* to the original problem (12)-(14) [5], [11]. It is used to incrementally update the activation durations

$$\bar{\delta}^{(i+1)} = \bar{\delta}^{(i)} + \alpha^{(i)}\Delta\bar{\delta}^{\star} \tag{15}$$

with a proper step size $\alpha^{(i)}$.

C. Projection of candidate points via optimization

Candidate sample points $\boldsymbol{x}_{(k+1)i} \in \mathcal{T}^{\star}_{(k+1)k}(\boldsymbol{x}^{\star}_{(k+1)j})$ are points located on the tangent plane in a local neighborhood around an anchor point $\boldsymbol{x}^{\star}_{(k+1)j}$. Since the latter is a point on the optimal surface $\mathcal{M}^{\star}_{(k+1)k}$, the optimal event function $|\Phi^{\star}_{(k+1)k}(\boldsymbol{x}_{(k+1)i})| \approx 0$ is expected to return approximately zero.

For polygonization of optimal switching surfaces, these candidate points must be successively projected onto $\mathcal{M}^{\star}_{(k+1)k}$ along the direction of the tangent normal $\boldsymbol{n}^{\star}(\boldsymbol{x}^{\star}_{(k+1)j})$ (see Fig. 3). Essentially, this projection is achieved by solving (12)-(14) via SQP, but with a slightly modified iterative procedure. Given a current guess $\bar{\delta}^{(i)} = \big(0,\ \delta_1^{(i)}\big)$ we can solve the associated SQP-LQR problem to obtain $\Delta\bar{\delta}^{\star}$. Now, instead of updating the first activation duration $\delta_0^{(i)}$, the candidate point is taken to be a decision variable and shifted along the tangent plane normal according to

$$\boldsymbol{x}^{(i+1)}_{(k+1)i} = \boldsymbol{x}^{(i)}_{(k+1)i} + \alpha^{(i)} \frac{\Delta\bar{\delta}^{\star}}{\boldsymbol{n}^{\mathrm{T}}(\boldsymbol{x}^{\star}_{(k+1)j})\boldsymbol{n}(\boldsymbol{x}^{\star}_{(k+1)j})}\ . \tag{16}$$

The second duration $\delta_1^{(i)}$ is updated as previously. Since candidate points are close to the true optimal surfaces, a good the initial guess $\bar{\delta}^{(0)}(\boldsymbol{x}_{(k+1)i})$ is available from the previous optimization and SQP corresponds to a second order method, the iteration typically converges to a stationary solution within a few steps.

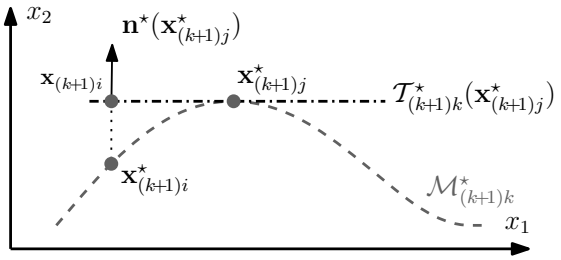

Fig. 3. Projection of candidate points onto $\mathcal{M}^{\star}_{(k+1)k}$.

Remark 5: Due to non-convexity of Prob. 1, it is not guaranteed that each projection optimization converges to the same local minimum of (4). By placing new candidate points on the corresponding tangent plane, the likelihood of converging to a different local optimum during the projection is at least small. A change in the local optimum causes a discontinuity in the optimal surface, which cannot be accurately represented through polygonization.

D. Determination of tangent planes via optimal perturbation feedback control

In a local neighborhood around $\boldsymbol{x}^{\star}_{(k+1)j}$, the tangent plane $\mathcal{T}^{\star}_{(k+1)k}(\boldsymbol{x}^{\star}_{(k+1)j})$ constitutes a fairly accurate representation of $\mathcal{M}^{\star}_{10}$. Hence, knowledge about the tangent plane can be successfully employed to mitigate the effects of small initial state uncertainties and disturbances. Triggering the mode transition $0 \to 1$ whenever a locally perturbed trajectory $\boldsymbol{x}(t)$ intersects with $\mathcal{T}^{\star}_{(k+1)k}(\boldsymbol{x}^{\star}_{(k+1)i})$ corresponds to the application of a locally optimal feedback correction to the nominal switching time $\tau^{\star}(\boldsymbol{x}^{\star}_{(k+1)j})$.

For ordinary discrete-time N-stage systems under the influence of arbitrary-but-small initial and terminal state perturbations $\Delta\boldsymbol{x}_0$ and $\Delta\boldsymbol{x}_N$, such a *locally* optimal linear perturbation feedback controller was proposed in [9]. This controller computes small input adjustments that preserve optimality up to first order. Thanks to the reformulation of Sect. IV-B, it is possible to extend this control scheme to bimodal switched-mode system with terminal inequality constraints. Due to its length, the proof of the following theorem is postpone to App. B.

Theorem 1: Given nominal optimal sequences $\bar{\delta}^{\star}, \bar{\boldsymbol{x}}^{\star}$ with respect to (12)-(14), a *neighboring extremal solution*

$$\bar{\delta}^{\star}(\boldsymbol{x}_0 + \Delta\boldsymbol{x}_0) = \bar{\delta}^{\star}(\boldsymbol{x}_0) + \Delta\bar{\delta}^{\star} \tag{17}$$

can be computed for arbitrary initial state perturbations $\Delta\boldsymbol{x}_0$ via linear state-feedback

$$\Delta\delta_k^{\star} = -\boldsymbol{K}_{k,\star}(\Delta\boldsymbol{x}_0)\boldsymbol{\xi}_k \tag{18}$$
$$\boldsymbol{\xi}_{k+1} = \boldsymbol{A}_{k,\star}\boldsymbol{\xi}_k + \boldsymbol{B}_{k,\star}\Delta\delta_k^{\star},\ \ \boldsymbol{\xi}_0 = \Delta\boldsymbol{x}_0\ . \tag{19}$$

The subscript star indicates that all matrices are evaluated along the optimal sequences $\bar{\delta}^{\star}, \bar{\boldsymbol{x}}^{\star}$.

The neighbouring extremal solution (17) satisfies the terminal constraints $\boldsymbol{\psi}(\boldsymbol{x}_2) = \mathbf{0}$, iff the switched system is locally controllable in a neighbourhood around the nominal trajectory. Note here that the optimal feedback gain $\boldsymbol{K}_{k,\star}(\Delta\boldsymbol{x}_0)$ is

a piecewise-constant function of the initial state $\boldsymbol{x}_0$ and the perturbation direction $\Delta\boldsymbol{x}_0$.

As stated in (18), the perturbation feedback law must be applied at the activation instant of each mode. By taking into account that the inverse state transition matrix $\boldsymbol{A}_k^{-1}$ maps local perturbations from the deactivation instant of a mode to its activation instant, it is possible modify the perturbation controller, such that it applies optimal adjustements to the nominal activation duration right before the termination of the corresponding mode. This modified perturbation controller defines the tangent planes $\mathcal{T}^{\star}_{(k+1)k}(\boldsymbol{x}^{\star}_{(k+1)j})$.

Theorem 2: The optimal perturbation control law (18) defines planes

$$\mathcal{T}^{\star}_{(k+1)k}(\boldsymbol{x}^{\star}_{k+1}) = \left\{\boldsymbol{x} \;:\; \boldsymbol{K}_{k,\star}\boldsymbol{A}^{-1}_{k,\star}\left(\boldsymbol{x}-\boldsymbol{x}^{\star}_{k+1}\right)=0\right\} \quad , \qquad (20)$$

which are anchored at the nominal switch point $\boldsymbol{x}^{\star}_{k+1}$ and are tangent to the optimal surfaces $\mathcal{M}^{\star}_{(k+1)k}$.

Proof: Small adjustments $\Delta\delta_k$ of the optimal activation duration are only critical, if $\delta^{\star}_k$ is close to zero. As long as the deviation $\Delta\boldsymbol{x}(t) = \boldsymbol{x}(t) - \boldsymbol{x}^{\star}(t)$ from the optimal trajectory is small, all optimal mode transitions occur in a vicinity of the optimal switch point $\boldsymbol{x}^{\star}_{k+1}$, when the switching condition

$$\begin{aligned}\Phi^{\star}_{(k+1)k}(\boldsymbol{x}^{\star}_{k+1}+\Delta\boldsymbol{x}_{k+1}) &= \Phi^{\star}_{(k+1)k}(\boldsymbol{x}^{\star}_{k+1}) + \frac{\mathrm{d}\Phi^{\star}_{(k+1)k}}{\mathrm{d}\boldsymbol{x}}(\boldsymbol{x}^{\star}_{k+1})\Delta\boldsymbol{x}_{k+1} + \text{h.o.t.}\\ &= \boldsymbol{K}_{k,\star}\boldsymbol{A}^{-1}_{k,\star}\Delta\boldsymbol{x}_{k+1} + \text{h.o.t.} = 0\end{aligned}$$

is satisfied. Provided that $\Delta\boldsymbol{x}_{k+1}$ is small, all higher order term can be neglected and the mode transition is optimally triggered, whenever the perturbation $\Delta\boldsymbol{x}_{k+1}$ is orthogonal to $\tilde{\boldsymbol{K}}_{k,\star}\boldsymbol{A}_{k,\star}$. Thus, the vector $\boldsymbol{n}_k^{\mathrm{T}} = \boldsymbol{K}_{k,\star}\boldsymbol{A}^{-1}_{k,\star}$ constitutes the normal to the hyperplane, which is tangent to $\mathcal{M}^{\star}_{(k+1)k}$. ■

E. Properties of optimal switching surfaces

It can be shown by tedious algebraic manipulations that $\boldsymbol{n}_k^{\mathrm{T}}\boldsymbol{B}_k = -1$ and $\|\boldsymbol{n}_k^{\mathrm{T}}\| < \infty$. Together, this guarantees, that optimal switching surfaces are always intersected transversally, which is critical for the validity of the resulting feedback controller. However, no conclusions about the length of $\boldsymbol{n}_k^{\mathrm{T}}$ nor its sensitivity $\partial\boldsymbol{n}_k^{\mathrm{T}}/\partial\boldsymbol{x}$ can be made. In the worst case, the optimal surfaces can have a strong curvature and the intersection could be nearly tangential.

Theo. 1 proves the stipulated property that the optimal event function is continuous and at least piecewise differentiable at all relevant points. This property is fundamental for convergence of $\tilde{\Phi}^{\star}_{10}$ to $\Phi^{\star}_{10}$ with decreasing mesh size [1]. Besides this convergence property, however, it is extremely difficult to derive a rigorous relation between the mesh size and the approximation precision. Such accuracy bounds require a strong insight into the problem at hand. Several heuristics have been developed to successively control the mesh size on the basis of curvature information [18], [10], but none of these methods give any guarantees concerning the accuracy.

V. EXAMPLE

Algorithm 1 was applied construct the optimal surface for a robot example, described in [8]. In this example, a unicylce has to reach a prespecified target from a given initial set, while avoiding an obstacle along its path. To achieve this objective, the unicycle can be switched among two different control strategies, namely "avoid-obstacle" and "approach-target". The corresponding mode dynamics, the cost functional and the parameter set are taken from [8].

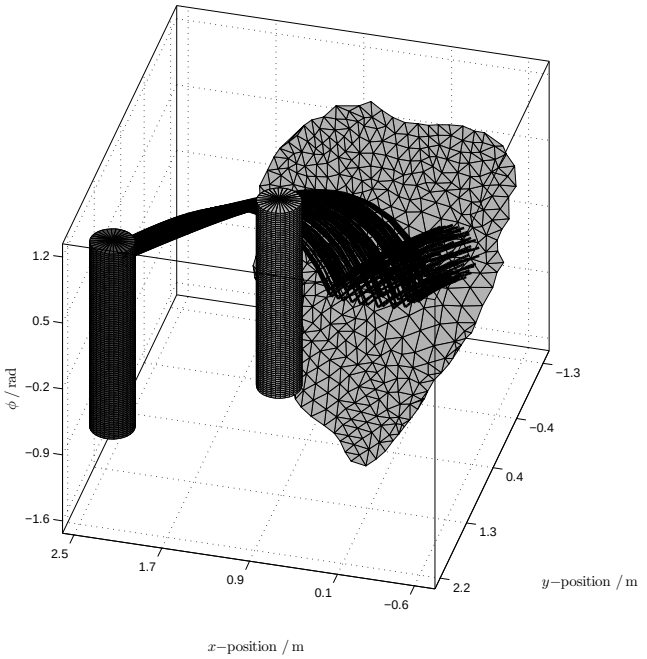

Fig. 4. Optimal switching surface for the robot example. As shown by the sample trajectories, the robot successfully avoids the obstacle and reaches the target at the end of its motion.

The situation considered here is the following: the robot starts inside the initial set $\mathcal{X}_0 = \{\boldsymbol{x} : \|\boldsymbol{x}\| = 0.25\}$ with the "avoid-obstacle" mode activated and is allowed to switch to the "approach-goal" mode whenever appropriate. As the terminal constraint, the robot must exactly stop at the target location, i.e. $\Psi(\boldsymbol{x}_2) = \|(x_1\ x_2)^{\mathrm{T}} - (x_{g1}\ x_{g2})^{\mathrm{T}}\| = 0$.

Fig. (4) depicts the computed optimal surface and a family of optimal trajectory in the state space. As observed, the unicycle successfully avoids the obstacle (light grey cylinder) for all trajectories. It operates in the "avoid-obstacle" mode for a short time, until it intersects the optimal surface $\mathcal{M}^{\star}_{10}$ (triangulated light grey patch). After switching to the "approach-goal" mode, it drives to the target (dark grey cylinder) on a curvy path.

A close inspection reveals that the triangulation of $\mathcal{M}10^{\star}$ results in mesh of nearly equilateral triangles, which is due to the low curvature of the surface. Being a consequence of the problem's non-convexity, the depicted patch corresponds at best to a locally optimal switching surface. Because of this, it is crucial to expand the surface always along the tangent planes at the boundary points in order to prevent discontinuities in the surface.

The computational effort to generate the optimal surface patch is overly acceptable. In total, it took less than a 1/10 of the time required to execute the switching time optimization for 100 sample trajectories starting from inside

$\mathcal{X}_0$. This approach is well suited for periodically switched systems.Hence, the off-line computation of optimal switching surfaces proves to be especially valuable for periodically operated systems, which execute the same mode transitions over and over again.

VI. CONCLUSION

This paper presents a novel off-line procedure for designing optimal switching surfaces, which enable an optimal closed-loop operation of a switched autonomous system with n-switches. Compared to the open-loop switching time optimal control, this closed-loop control approach is less sensitive to disturbances, model-mismatches and uncertainties of the initial state. Moreover, optimality is guaranteed for a complete family of trajectories, not just a single one. This approach is well suited for periodically switched systems.

The proposed methodology is based on the successive polygonization of the optimal surfaces by means of the marching triangle algorithm. It allows to concentrate the surface reconstruction exclusively to the state space region, which is relevant for the system's operation, in order to maintain the computational effort as low as possible. This is crucial for the practical applicability of the approach.

All results presented in the paper can be extended to autonomous hybrid systems, with N controlled and autonomous switches as well as state jumps.

VII. ACKNOWLEDGEMENTS

The work of A. Schild and J. Lunze is supported by the German Research Foundation (LU462/21-3) and the German Academic Exchange Service (D/08/45420). The work by M. Egerstedt and X. Ding was funded by the US national science foundation (0509064).

REFERENCES

[1] E. L. Allgower and K. Georg. Estimates for piecewise linear approximations of implicitly defined manifolds. *Appl. Math. Lett.*, 1(5):1–7, 1989.

[2] E. L. Allgower and K. Georg. Numerical path following. In *Handbook of Numerical Analysis. Volume V. Techniques of Scientific Computing. (Part 2)*. Elsevier, 1997.

[3] H. Axelsson, M. Boccadoro, M. Egerstedt, P. Valigi, and Y. Wardi. Optimal mode-switching for hybrid systems with varying initial states. *Journal of Nonlinear Analysis: Hybrid Systems and Applications*, 2:167–186, 2008.

[4] R. Bellman. *Dynamic Programming*. Dover, 2003.

[5] D.P. Bertsekas. *Nonlinear Programming*. Athena Scientific, 2nd edition, 2003.

[6] J. Bloomenthal. Implicit surfaces. In *Encyclopedia of Computer Science and Technology, Volume 44*. Marcel Dekker, 2001.

[7] M. Boccadoro, M. Egerstedt, P. Valigi, and Y. Wardi. Beyond the construction of optimal switching surfaces for autonomous hybrid systems. In *Proc. of ADHS*, pages 101–105, Alghero, Italy, 2006.

[8] M. Boccadoro, Y. Wardi, M. Egerstedt, and E. Verriest. Optimal control of switching surfaces in hybrid systems. *Discrete Event Dynamic Systems*, 15(4):433–448, 2005.

[9] A.E. Bryson and Y.-C. Ho. *Applied Optimal Control - Optimization, Estimation and Control*. Taylor and Francis, 1975.

[10] B.R. de Araujo and J.A.P. Jorge. Curvature dependent polygonization of implicit surfaces. In *XVII Brazilian Symposium on Computer Graphics and Image Processing (SIBGRAPI'04)*, 2004.

[11] C. R. Dohrmann and R. D. Robinett. Dynamic programming method for constrained discrete-time optimal control. *JOTA*, 101:259–283, 1999.

[12] M. Egerstedt, S.-I. Azuma, and Y. Wardi. Optimal timing control of switched linear systems based on partial information. *Nonlinear Analysis: Theory, Methods and Applications*, 65(9):1736–1750, 2006.

[13] M. Egerstedt, Y. Wardi, and H. Axelsson. Transition-time optimization for switched-mode dynamical systems. *IEEE Transaction on Automatic Control*, 51:110–115, 2006.

[14] A. Giua, C. Seatzu, and C. van der Mee. Optimal control of switched autonomous linear systems. In *Proc. 40th Conf. on Decision and Control*, Florida, USA, 2001.

[15] E. Hartmann. A marching method for the triangulation of surfaces. *The Visual Computer*, 14:95–108, 1998.

[16] M. E. Henderson. Multiple parameter continuation: computing implicitly defined k-manifolds. *International Journal of Bifurcation and Chaos*, 12(3):451–476, 2002.

[17] A. Hilton, A.J. Stoddart, J. Illingworth, and T. Windeatt. Marching triangles: range image fusion for complex object modelling. In *Proceedings of teh International Conference on Image Processing*, 1990.

[18] T. Karkanis and A.J. Stewart. Curvature-dependent triangulation of implicit surfaces. *IEEE COMPUTER GRAPHICS AND APPLICATIONS*, 21:60–69, 2001.

[19] J. Moon, Y. Wardi, and E. Kamen. Optimal release times in single-stage manufacturing systems with finite production inventory. In *Proc. 41st IEEE Conference on Decision and Control*, volume 3, pages 2506–2511, 10–13 Dec. 2002.

[20] M. S. Shaikh and P. E. Caines. On the hybrid optimal control problem: Theory and algorithms. 52(9):1587–1603, Sept. 2007.

[21] C. K. Tse. *Complex Behavior of Switching Power Converters*. CRC Press, USA, 2004.

[22] Y. Wardi, X.C. Ding, M. Egerstedt, and S.-I. Azuma. On-line optimization of switched-mode systems: Algorithms and convergence properties. In *Proc. on 46th IEEE Conference on Decision and Control*, 2007.

[23] X. Xu and P.J. Antsaklis. Optimal control of switched systems via nonlinear optimization based on direct differentiations of value functions. *International Journal of Control*, 75:1406–1426, 2002.

APPENDIX

A. First and second order partial derivatives of the discretized dynamics and the discrete Hamiltonian

Given any pair $(\bar{\delta}, \bar{\boldsymbol{x}})$ consistent with (13), the Hamiltonian of a discrete time optimal control problem is defined as

$$H_k(\boldsymbol{x}_k, \delta_k, \boldsymbol{p}_{k+1}) = \boldsymbol{p}_{k+1}^{\mathrm{T}} \boldsymbol{h}(\boldsymbol{x}_k, \delta_k) + g_k(\boldsymbol{x}_k, \delta_k) \qquad (21)$$

and the costate $\boldsymbol{p}_{k+1}$ is determined by backward iteration

$$\boldsymbol{p}_k^{\mathrm{T}} = \frac{\partial H_k}{\partial \boldsymbol{x}}(\boldsymbol{x}_k, \delta_k, \boldsymbol{p}_{k+1}) = \boldsymbol{p}_{k+1}^{\mathrm{T}} \boldsymbol{A}_k + \boldsymbol{a}_k, \quad \boldsymbol{p}_N^{(i),\mathrm{T}} = \boldsymbol{v}^{(i),\mathrm{T}} \quad . \qquad (22)$$

From these definitions the following exact expression for the partial derivatives

$$\boldsymbol{A}_k = \frac{\partial \boldsymbol{h}_k}{\partial \boldsymbol{x}}(\boldsymbol{x}_k, \delta_k) = \boldsymbol{Z}_k(\delta_k) \tag{23}$$

$$\boldsymbol{a}_k = \frac{\partial g_k}{\partial \boldsymbol{x}}(\boldsymbol{x}_k, \delta_k) = \int_0^{\delta_k} \frac{\partial L_k}{\partial \boldsymbol{x}}(\boldsymbol{\zeta}(t))\, \boldsymbol{Z}_k(t)\, \mathrm{d}t + \frac{\partial \phi_k}{\partial \boldsymbol{x}}(\boldsymbol{x}_k \tag{24}$$

$$\boldsymbol{B}_k = \frac{\partial \boldsymbol{h}_k}{\partial \delta}(\boldsymbol{x}_k, \delta_k) = \boldsymbol{f}_k(\boldsymbol{x}_{k+1}) \tag{25}$$

$$\boldsymbol{b}_k = \frac{\partial g_k}{\partial \delta}(\boldsymbol{x}_k, \delta_k) = L_k(\boldsymbol{x}_{k+1}) \tag{26}$$

$$\boldsymbol{Q}_k = \frac{\partial^2 H_k}{\partial \boldsymbol{x}^2}(\boldsymbol{x}_k^{(i)}, \delta_k^{(i)}, \boldsymbol{p}_{k+1}^{(i)}), \quad \boldsymbol{C}_k = \frac{\partial \boldsymbol{f}_k}{\partial \boldsymbol{x}}\left(\boldsymbol{x}_{k+1}^{(i)}\right) \tag{27}$$

$$\boldsymbol{M}_k = \frac{\partial H_k^2}{\partial \boldsymbol{x} \partial \delta}(\boldsymbol{x}_k^{(i)}, \delta_k^{(i)}, \boldsymbol{p}_{k+1}^{(i)}) = \left(\frac{\partial L}{\partial \boldsymbol{x}}\left(\boldsymbol{x}_{k+1}^{(i)}\right) + \boldsymbol{p}_{k+1}^{(i),\mathrm{T}} \boldsymbol{C}_k\right) \boldsymbol{A}_k \tag{28}$$

$$\boldsymbol{R}_k = \frac{\partial H_k^2}{\partial \delta^2}(\boldsymbol{x}_k^{(i)}, \delta_k^{(i)}, \boldsymbol{p}_{k+1}^{(i)}) = \left(\frac{\partial L}{\partial \boldsymbol{x}}\left(\boldsymbol{x}_{k+1}^{(i)}\right) + \boldsymbol{p}_{k+1}^{(i),\mathrm{T}} \boldsymbol{C}_k\right) \boldsymbol{B}_k \tag{29}$$

$$\boldsymbol{C}_I = \frac{\partial \boldsymbol{\psi}}{\partial \boldsymbol{x}}(\boldsymbol{x}_N^{(i)}), \quad \boldsymbol{d}_I = \boldsymbol{\psi}(\boldsymbol{x}_N^{(i)}) \ . \tag{30}$$

can be derived, which are needed for solving the problem (12)-(14) via SQP.

B. Proof of Theorem 1

The proof of Theo. 1 requires an intermediate result, which is obtained by extending the perturbation feedback controller for N-stage systems with a terminal equality constraints presented in [9] to the switched-mode systems.

Lemma 1: [9] Given nominally optimal sequences $\bar{\delta}^\star$ and $\bar{\boldsymbol{x}}^\star$ with respect to (12)-(14), a neighboring extremal solution (17) can be computed for arbitrary initial and terminal state perturbations $\Delta\boldsymbol{x}_0$ and $\Delta\boldsymbol{x}_2$ via the affine state-feedback

$$\Delta\delta_k^\star = -\tilde{\boldsymbol{K}}_{k,\star}\boldsymbol{\xi}_k - \boldsymbol{\gamma}_{k,\star}^{\mathrm{T}}\Delta\boldsymbol{x}_2 \tag{31}$$

$$\boldsymbol{\xi}_{k+1} = \boldsymbol{A}_{k,\star}\boldsymbol{\xi}_k + \boldsymbol{B}_{k,\star}\Delta\delta_k, \quad \boldsymbol{\xi}_0 = \Delta\boldsymbol{x}_0^\star \tag{32}$$

with $\beta_{k,\star} = \left(\boldsymbol{R}_{k,\star} + \boldsymbol{B}_{k,\star}^{\mathrm{T}}\boldsymbol{P}_{k+1,\star}\boldsymbol{B}_{k,\star}\right)^{-1}$ and matrices and vectors

$$\boldsymbol{\rho}_{k,\star}^{\mathrm{T}} = \boldsymbol{M}_{k,\star} + \boldsymbol{B}_{k,\star}^{\mathrm{T}}\boldsymbol{P}_{k+1,\star}\boldsymbol{A}_{k,\star}, \quad \boldsymbol{\gamma}_k^{\mathrm{T}} = \beta_{k,\star}\boldsymbol{B}_{k,\star}\boldsymbol{U}_{k+1,\star}\boldsymbol{U}_{k,\star}^\dagger \tag{33}$$

$$\tilde{\boldsymbol{K}}_{k,\star} = \beta_{k,\star}\left(\boldsymbol{\rho}_{k,\star}^{\mathrm{T}} - \boldsymbol{B}_{k,\star}^{\mathrm{T}}\boldsymbol{U}_{k+1,\star}\boldsymbol{V}_{k,\star}^\dagger\boldsymbol{U}_{k,\star}^{\mathrm{T}}\right) \tag{34}$$

$$\boldsymbol{P}_{k,\star} = \boldsymbol{Q}_{k,\star} + \boldsymbol{A}_{k,\star}^{\mathrm{T}}\boldsymbol{P}_{k+1,\star}\boldsymbol{A}_{k,\star} + \boldsymbol{\rho}_{k,\star}\beta_{k,\star}\boldsymbol{\rho}_{k,\star}^{\mathrm{T}}, \quad \boldsymbol{P}_{2,\star} = \boldsymbol{0} \tag{35}$$

$$\boldsymbol{U}_{k,\star} = \boldsymbol{A}_{k,\star}^{\mathrm{T}}\boldsymbol{U}_{k+1,\star} - \boldsymbol{\rho}_{k,\star}\beta_{k,\star}\boldsymbol{B}_{k,\star}^{\mathrm{T}}\boldsymbol{U}_{k+1,\star}, \quad \boldsymbol{U}_{2,\star} = -\boldsymbol{I} \tag{36}$$

$$\boldsymbol{V}_{k,\star} = \boldsymbol{V}_{k+1,\star} + \boldsymbol{U}_{k+1,\star}^{\mathrm{T}}\boldsymbol{B}_{k,\star}\beta_{k,\star}\boldsymbol{B}_{k,\star}^{\mathrm{T}}\boldsymbol{U}_{k+1,\star}, \quad \boldsymbol{V}_{2,\star} = \boldsymbol{0} \tag{37}$$

evaluated along the optimal sequences $\bar{\delta}^\star$, $\bar{\boldsymbol{x}}^\star$. The superscript † denotes the Penrose-Moore pseudo-inverse.

If the terminal constraints are relaxed to inequality constraints that enforce a terminal set $\mathcal{X}_T$, as it is the case for (12)-(13), the terminal perturbation $\Delta\boldsymbol{x}_2$ constitutes a constrained decision variable itself. Its optimal value is to be determined via a nested quadratic optimization problem.

In this case substitute the feedback (31) into the quadratic cost function

$$\Delta\tilde{J}(\Delta\bar{\delta}) = \sum_{k=0}^{1} \tfrac{1}{2}\boldsymbol{\xi}_k^{\mathrm{T}}\boldsymbol{Q}_k\boldsymbol{\xi}_k + \boldsymbol{a}_k^{\mathrm{T}}\boldsymbol{\xi}_k + \Delta\delta_k^{\mathrm{T}}\boldsymbol{M}_k\boldsymbol{\xi}_k + \tfrac{1}{2}\Delta\delta_k^{\mathrm{T}}\boldsymbol{R}_k\Delta\delta_k + \boldsymbol{b}_k^{\mathrm{T}}\Delta\delta_k$$

to be minimized at each SQP step and also into (19). This yields the adjoint quadratic optimization problem

$$\min_{\boldsymbol{\xi}_2} \ \Delta\tilde{J}(\boldsymbol{\xi}_2) = \sum_{k=0}^{1} \tfrac{1}{2}\boldsymbol{\xi}_k^{\mathrm{T}}\tilde{\boldsymbol{Q}}_k\boldsymbol{\xi}_k + \boldsymbol{\xi}_2^{\mathrm{T}}\tilde{\boldsymbol{M}}_k\boldsymbol{\xi}_k + \tfrac{1}{2}\boldsymbol{\xi}_2^{\mathrm{T}}\tilde{\boldsymbol{R}}_k\boldsymbol{\xi}_2 \tag{38}$$

$$\boldsymbol{\xi}_{k+1} = \left(\boldsymbol{A}_{k,\star} - \boldsymbol{B}_{k,\star}\tilde{\boldsymbol{K}}_{k,\star}\right)\boldsymbol{\xi}_k + \boldsymbol{B}_k\boldsymbol{\gamma}_{k,\star}^{\mathrm{T}}\boldsymbol{\xi}_2, \quad \boldsymbol{\xi}_0 = \Delta\boldsymbol{x}_0 \tag{39}$$

$$\boldsymbol{C}_{I,a}\boldsymbol{\xi}_2 \leq 0 \ . \tag{40}$$

with costs in terms of

$$\boldsymbol{K}_{k,\star} = \tilde{\boldsymbol{K}}_{k,\star} + 2\tilde{\boldsymbol{\gamma}}_k^{\mathrm{T}}\boldsymbol{Y}_{k,\star}^\dagger\boldsymbol{X}_{k,\star}, \quad \boldsymbol{W}_{2,\star} = \boldsymbol{X}_{2,\star} = \boldsymbol{Y}_{2,\star} = \boldsymbol{0} \tag{41}$$

$$\tilde{\boldsymbol{\gamma}}_k = \boldsymbol{C}_{I,\perp}(\Delta\boldsymbol{x}_0)\boldsymbol{\gamma}_k \tag{42}$$

$$\boldsymbol{W}_{k,\star} = \tilde{\boldsymbol{Q}}_{k,\star} + \left(\boldsymbol{A}_{k,\star} - \boldsymbol{B}_{k,\star}\tilde{\boldsymbol{K}}_{k,\star}\right)^{\mathrm{T}}\boldsymbol{W}_{k+1\star}\left(\boldsymbol{A}_{k,\star} - \boldsymbol{B}_{k,\star}\tilde{\boldsymbol{K}}_{k,\star}\right) \tag{43}$$

$$\boldsymbol{X}_{k,\star} = \tilde{\boldsymbol{M}}_{k,\star} + \left(\tilde{\boldsymbol{\gamma}}_k\boldsymbol{B}_{k,\star}^{\mathrm{T}}\boldsymbol{W}_{k+1,\star} + \boldsymbol{X}_{k+1,\star}\right)\left(\boldsymbol{A}_{k,\star} - \boldsymbol{B}_{k,\star}\tilde{\boldsymbol{K}}_{k,\star}\right) \tag{44}$$

$$\boldsymbol{Y}_{k,\star} = \tilde{\boldsymbol{R}}_{k,\star} + \boldsymbol{Y}_{k+1,\star} + \left(\tilde{\boldsymbol{\gamma}}_{k,\star}\boldsymbol{B}_{k,\star}^{\mathrm{T}}\tilde{\boldsymbol{R}}_{k+1,\star} + 2\boldsymbol{X}_{k+1,\star}\right)\boldsymbol{B}_{k,\star}\tilde{\boldsymbol{\gamma}}_{k,\star}^{\mathrm{T}} \tag{45}$$

$$\tilde{\boldsymbol{Q}}_{k,\star} = \boldsymbol{Q}_{k,\star} + \tilde{\boldsymbol{K}}_{k,\star}^{\mathrm{T}}\left(\boldsymbol{R}_{k,\star}\tilde{\boldsymbol{K}}_{k,\star} - \boldsymbol{M}_{k,\star}\right) \tag{46}$$

$$\tilde{\boldsymbol{M}}_{k,\star} = \tilde{\boldsymbol{\gamma}}_{k,\star}\left(\boldsymbol{R}_{k,\star}\tilde{\boldsymbol{K}}_{k,\star} - \boldsymbol{M}_{k,\star}\right), \quad \tilde{\boldsymbol{R}}_{k,\star} = \tilde{\boldsymbol{\gamma}}_{k,\star}\boldsymbol{R}_{k,\star}\tilde{\boldsymbol{\gamma}}_{k,\star}^{\mathrm{T}} \tag{47}$$

and the decision variable $\boldsymbol{\xi}_2$. The columns of $\boldsymbol{C}_{I,\perp}(\Delta\boldsymbol{x}_0)$ in (42) span the null space of $\boldsymbol{C}_{I,a}$, i.e. the set of *active* linearized inequality constraints. The j-th inequality constraint is denoted as active, iff $\psi_j(\boldsymbol{x}_2^\star) = 0$ holds for the nominal terminal point $\boldsymbol{x}_2^\star$ and the infinitesimal perturbation $\Delta\boldsymbol{x}_0$ will not cause the constraint to become inactive. Clearly, the optimal terminal perturbation must lie inside $\boldsymbol{C}_{I,\perp}(\Delta\boldsymbol{x}_0)$. Moreover, the number of inequality constraints is finite, such that $\boldsymbol{C}_{I,\perp}(\Delta\boldsymbol{x}_0)$ is a piecewise constant function.

By recursive application of dynamic programming to (38), (39), the expressions (43)-(45) are obtained together with optimal value $\Delta\boldsymbol{x}_2^\star = -2\boldsymbol{Y}_k^\dagger\boldsymbol{X}_k\boldsymbol{\xi}_k$. Substituting this feedback into (31) yields (18) and thus (41). As a consequence of (42), the optimal feedback $\boldsymbol{K}_{k,\star} = \boldsymbol{K}_{k,\star}(\boldsymbol{x}_0, \Delta\boldsymbol{x}_0)$ is also *piecewise constant*. Nevertheless, the structure of the optimal perturbation feedback (18) is still linear for a particular initial perturbation $\Delta\boldsymbol{x}_0$.

Remark 6: The dynamic programming approach, which is exploited in Theo. 1, may not be the most efficient way to solve a constrained quadratic optimization problem (12)-(14), but it provides valuable insight into the problem structure. Linearity of the perturbation feedback controller is necessary and sufficient for extracting the tangent plane information at a candidate point $\boldsymbol{x}_{ki}^\star$ as a by-product of the preceding projection.